Cell Reports Medicine, Volume *3*

Supplemental information

Patient-derived models of brain metastases recapitulate human disseminated disease

Claudia C. Faria, Rita Cascão, Carlos Custódia, Eunice Paisana, Tânia Carvalho, Pedro Pereira, Rafael Roque, José Pimentel, José Miguéns, Isidro Cortes-Ciriano, and João T. Barata

SUPPLEMENTAL INFORMATION

Supplementary Table 1. Summary of the clinical data of BMs patients and experimental results from PDX and PDC models.

Patient										PDX models								PDC
										Subcutaneous				Intracardiac				
Pt. No.	Sample ID	Gender	Age	Primary tumor	Location (ST/IT)	Specific location	No. of BMs	Previous Radiation (RT/RS)	Overall survival (months)	Engrafted	Latency time (days)	Metastases	CNS Metastases	Engrafted	Survival (Days)	Metastases	CNS Metastases	Yes/No
1	MET-CF29	F	70	Bladder	ST	Skull	1	No	7.4	Yes	31 (24-67)	No	No	Yes	45 (42-67)	Yes	Yes (B)	Yes
2	MET-CF30	M	72	Lung	IT	Cerebellar hemisphere	2	No	5.8	Yes	69 (58-76)	No	No	Yes	144 (130-158)	Yes	No	Yes
3	MET-CF32	M	80	Bladder	ST	Temporal	2	No	16.7	Yes	70	No	No	NP	-	-	-	No
4	MET-CF38	M	49	Lung	IT	Cerebellar hemisphere	1	No	10.4	Yes	20 (18-29)	Yes	No	NP	-	-	-	No
5	MET-CF58	M	65	Lung	ST	Parietal	2	No	7.4	Yes	22 (18-47)	Yes	No	NP	-	-	-	No
6	MET-CF63	F	44	Breast	ST	Fronto-parietal	2	No	10.1	No	-	-	-	-	-	-	-	No
7	MET-CF65	M	25	Osteosarcoma	ST	Frontal	1	No	2.5	Yes	20 (22-30)	No	No	Yes	64 (61-72)	Yes	No	Yes
8	MET-CF66	F	66	Lung	ST	Frontal	1	No	15	Yes	31 (24-35)	Yes	Yes (LM)	Yes	175	Yes	No	No
9	MET-CF67	M	54	Lung	IT	Cerebellar hemisphere	1	RS	20.3	No	-	-	-	-	-	-	-	No
10	MET-CF68	M	59	Lung	ST	Frontal	1	No	19.3	Yes	26 (24-35)	Yes	No	Yes	65 (63-141)	Yes	No	Yes
11	MET-CF69	M	76	Melanoma	ST	Frontal	3	No	1.2	Yes	33 (38-46)	Yes	No	Yes	70 (60-75)	Yes	Yes (B+LM)	Yes
12	MET-CF70	F	80	Colon	IT	Vermis	1	No	8.1	Yes	34 (28-39)	Yes	No	Yes	83 (80-95)	Yes	Yes (B+LM)	Yes
13	MET-CF71	F	41	Nasosinusal	ST	Skull	1	No	17.8	No	-	-	-	-	-	-		No
14	MET-CF73	M	60	Renal	ST	Occipital	1	No	16.9	No	-	-	-	-	-	-	-	No
15	MET-CF74	M	59	Renal	ST	Orbital	1	No	4.1	No	-	-	-	-	-	-	-	No
16	MET-CF75	F	58	Colon	IT	Cerebellar hemisphere	1	No	2.4	Yes	46 (46-183)	No	No	No	-	-	-	Yes
17	MET-CF76	F	62	Lung	ST	Frontal	3	RT	16.8	No	-	-	-	-	-	-	-	No
18	MET-CF78	M	61	Lung	IT	Cerebellar hemisphere	2	No	6.5	Yes	26 (21-37)	Yes	Yes (LM)	Yes	77 (61-88)	Yes	No	Yes
19	MET-CF79	F	64	Lung	ST	Occipital	1	RS	10.3	Yes	62 (58-74)	No	No	Yes	145 (11-289)	Yes	No	No
20	MET-CF80	M	64	Lung	IT	Vermis	1	No	3.5	Yes	61 (40-102)	Yes	No	NP	-	-	-	Yes
21	MET-CF81	F	67	Endometrium	IT	Cerebellar hemisphere	9	No	1.5	Yes	33 (29-44)	Yes	No	Yes	131 (76-163)	Yes	Yes (B)	Yes
22	MET-CF82	M	72	Colon	ST	Temporal	1	No	6.1	Yes	62 (47-74)	Yes	No	Yes	186 (72-199)	Yes	-	Yes
23	MET-CF83	F	68	Breast	IT	Vermis	1	No	11.7	No	-	-	-	-	-	-	-	No
24	MET-CF84	F	54	Breast	IT	Cerebellar hemisphere	2	No	6.3	No	-	Yes	No	-	-	-	-	No
25	MET-CF85	M	73	Lung	ST	Frontal	2	RS	11.4	No	-	Yes	No	-	-	-	-	No
26	MET-CF87	M	67	Lung	ST	Temporal	1	No	11.3	Yes	45 (43-100)	Yes	No	Yes	114 (10-144)	Yes	Yes (B)	Yes
27	MET-CF88	M	55	Prostate	ST	Frontal	2	No	4.9	Yes	92 (64-166)	No	No	No	-	-	-	Yes
28	MET-CF89	M	81	Colon	IT	Cerebellar hemisphere	3	No	4.9	Yes	26 (22-34)	No	No	Yes	83 (64-92)	Yes	Yes (B)	Yes
29	MET-CF90	M	68	Lung	IT	Vermis	1	No	1.1	Yes	78	Yes	Yes (LM)	NP	-	-	-	No
30	MET-CF92	M	73	Lung	ST	Temporal	1	No	9.6	Yes	120	No	No	NP	-	-	-	No
31	MET-CF93	M	63	Lung	IT	Cerebellar hemisphere	1	No	6.2	No	-	-	-	-	-	-	-	No
32	MET-CF94	M	47	Lung	ST	Frontal	2	RS	6.1	No	-	-	-	-	-	-	-	No
33	MET-CF95	M	65	Lung	ST	Temporal	2	No	4.9	No	-	-	-	-	-	-	-	No
34	MET-CF96	F	55	Breast	ST	Parietal	3	No	3.4	Yes	65 (58-72)	No	No	NP	-	-	-	No
35	MET-CF97	F	81	Colon	ST	Temporal	2	No	3.0	Yes	75	No	No	NP	-	-	-	No

PDX: Patient-derived xenograft; PDC: Patient-derived culture; ST: Supratentorial; IT: Infratentorial; RT: Radiotherapy; RS: Radiosurgery; CNS: Central nervous system; B: Brain; LM: Leptomeninges; NP: Not performed. All values are presented as median with interquartile range. Related to Figure 1.

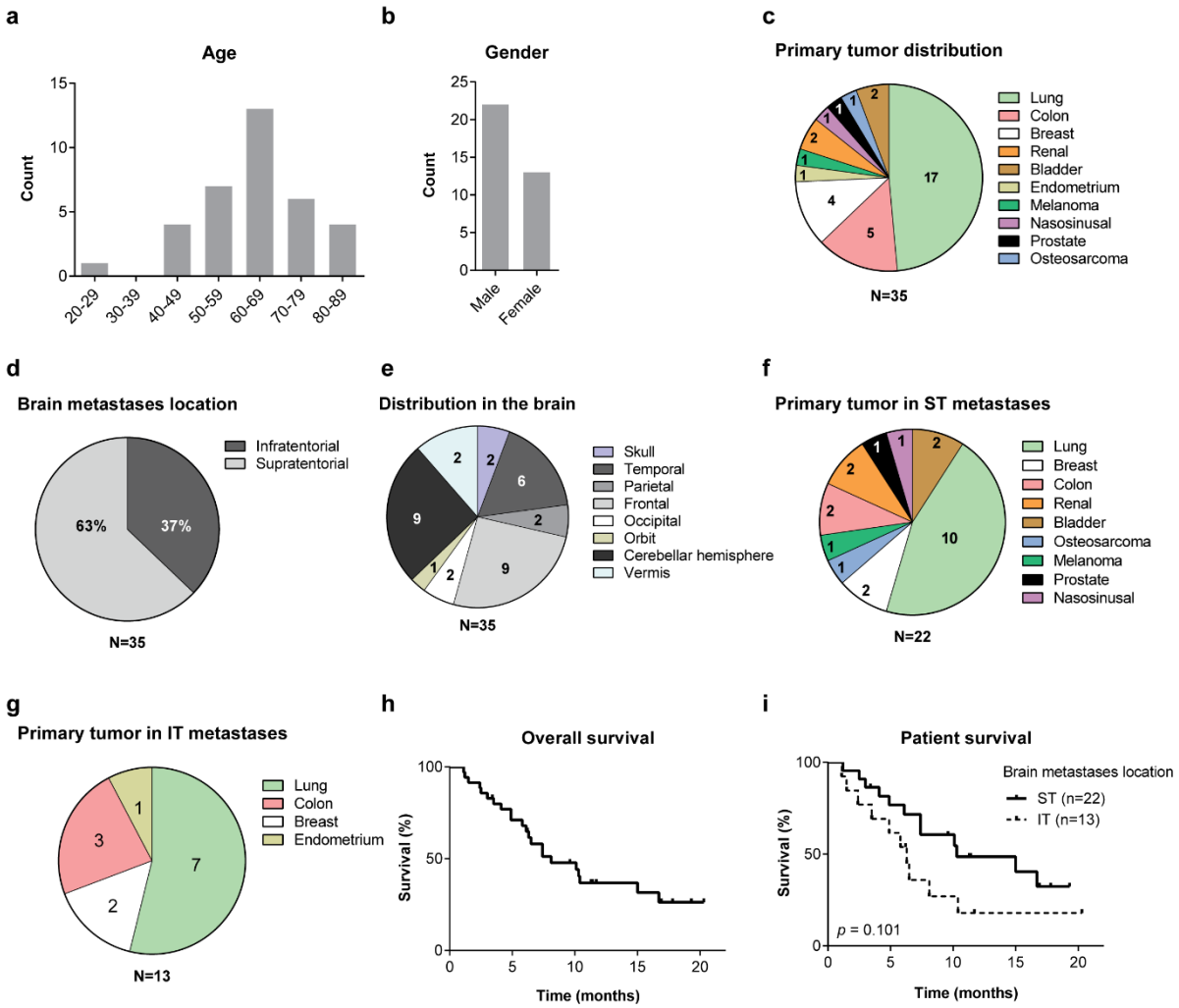

Supplementary Figure 1. Clinical characterization of the cohort of patients with BMs.
(**A**) Age of patients at the time of BMs surgery. (**B**) Gender distribution. (**C**) Distribution of patients according to the primary tumor. (**D**) Percentage of BMs in the supratentorial and infratentorial compartments. (**E**) Anatomical location of BMs. (**F-G**) Distribution of primary tumors according to the location in the intracranial compartments. (**H**) Overall survival of patients upon diagnosis of BMs. (**I**) Patient overall survival according to the metastases location in the intracranial compartments. ST: Supratentorial; IT: Infratentorial. Differences were considered statistically significant for p-values<0.05, according to the Log-rank (Mantel-Cox) test. Related to Figure 1.

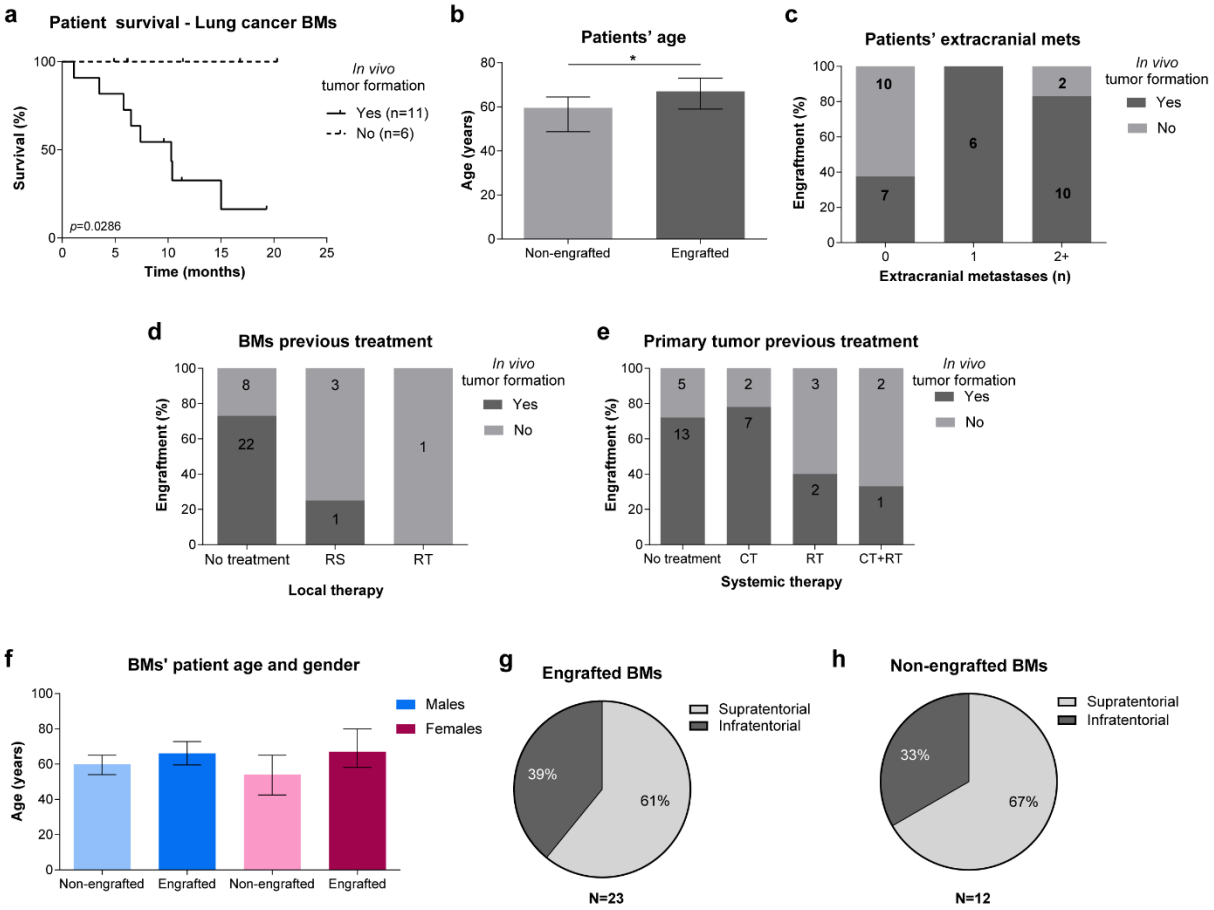

Supplementary Figure 2. Impact of clinical features on BMs engraftment.
(**A**) The *in vivo* tumorigenic potential of lung cancer BMs surgical samples correlates with patient poor survival (p=0.0286). (**B**) Engrafted samples derived from significantly older patients (p=0.0228). (**C**) Samples derived from patients displaying one or more extracranial metastases seem to have better engraftment ability. (**D**) BM local treatment seem to decrease engraft ability. (**E**) Treatment to the primary tumor with radiotherapy seems to decrease the ability of BMs to engraft in mice. (**F**) Comparison of patient median age for both engrafted vs non-engrafted samples by gender. (**G** and **H**) Distribution of BMs between supratentorial (ST) and infratentorial (IT) compartments for both engrafted and non-engrafted samples. Differences were considered statistically significant for p-values<0.05, according to an unpaired non-parametric Mann-Whitney test and to the Log-rank (Mantel-Cox) test. Related to Figure 1.

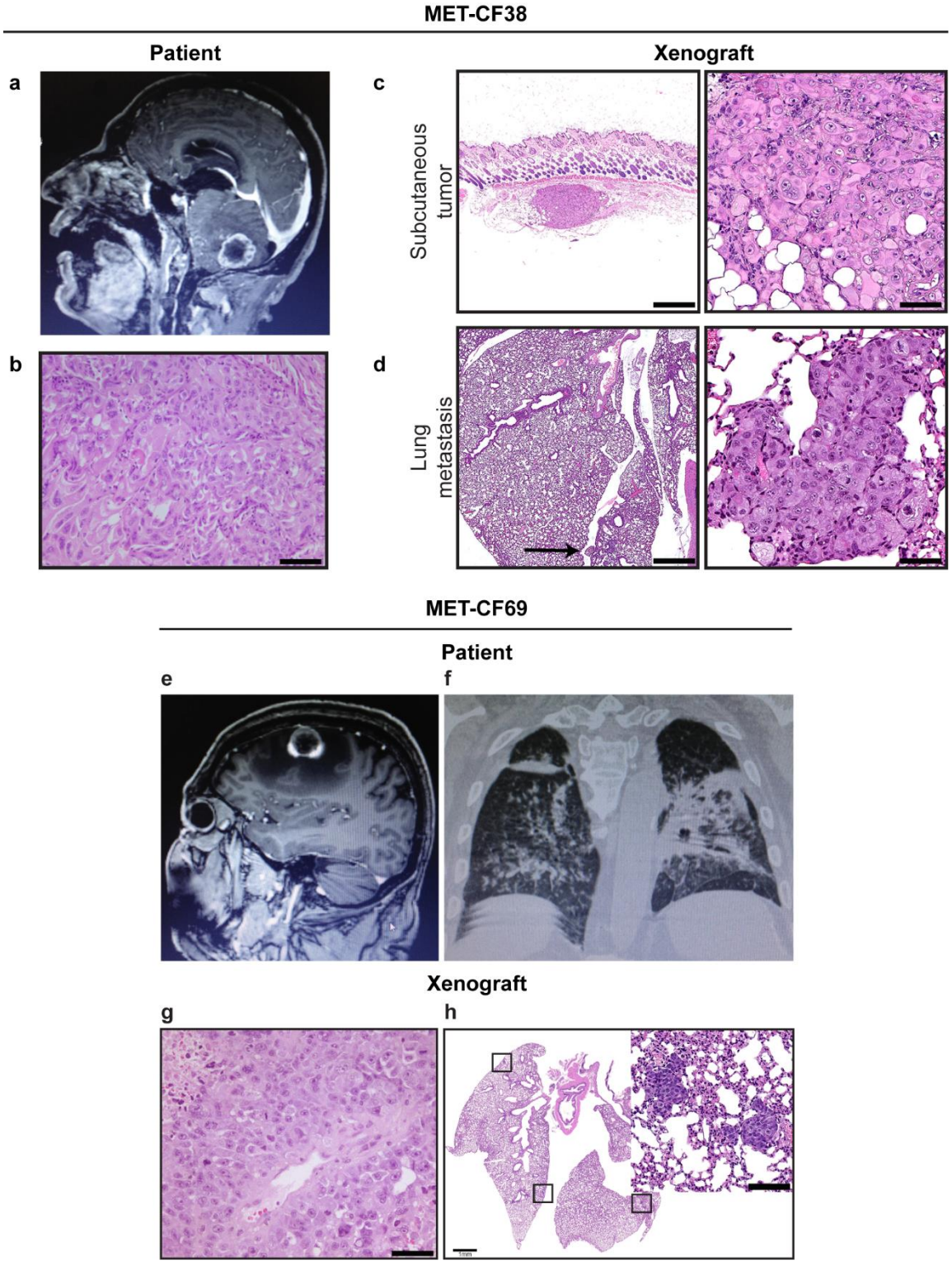

Supplementary Figure 3. Comparison of clinical cases and their matched subcutaneous PDXs models. Representative clinical case of a 49 years-old male patient with a stage IV lung adenocarcinoma where the BM (MET-CF38) xenografted in the mice flank originated spontaneous metastases in the lungs of the PDX. (**A**) Magnetic Resonance Imaging (MRI) of the brain, sagittal T1 contrast-enhanced sequence, showing a BM in the cerebellum. (**B**) H&E staining of the patient BM. (**C**) Corresponding H&E staining of the mouse flank xenograft. (**D**) Exclusive dissemination to the mouse lungs through passaging. Arrow indicates metastasis's location.
Representative clinical case of a 76 years-old male patient with metastatic melanoma to the brain (MET-CF69) and to the lungs, where the xenografted BM originated spontaneous metastases in the mice lungs. (**E**) Brain MRI, sagittal T1 contrast-enhanced, showing a left frontal BM. (**F**) Computed Tomography (CT) scan of the patient's lungs showing a diffuse infiltration by cancer cells. (**G**) H&E staining of the patient BM (20x). (**H**) H&E staining of the mice lungs exhibiting multiple metastases (squares). Scale bars: (B) 50µm, (C) 1mm and 50µm, (D) 1mm and 50µm, (G) 50µm, (H) 1mm. Related to Figure 2.

Supplementary Table 2. Matched patient and mice metastatic sites in subcutaneous PDX models.

Primary tumor	Sample ID	Metastases location									
		CNS	Lungs	Liver	Spleen	Kidney	Intraperit.	Lymph nodes	Soft tissues	Gonads	Bone/ Bone marrow
Lung	MET-CF38										
	MET-CF58										
	MET-CF66										
	MET-CF68										
	MET-CF78										
	MET-CF80										
	MET-CF85										
	MET-CF87										
	MET-CF90										
Melanoma	MET-CF69										
Colon	MET-CF70										
	MET-CF82										
Endometrium	MET-CF81										
Breast	MET-CF84										

Red - organs with tumor involvement in the patient; Green - organs with tumor involvement in the mouse; Yellow - organs with tumor involvement in both patient and mouse. Related to Figure 2.

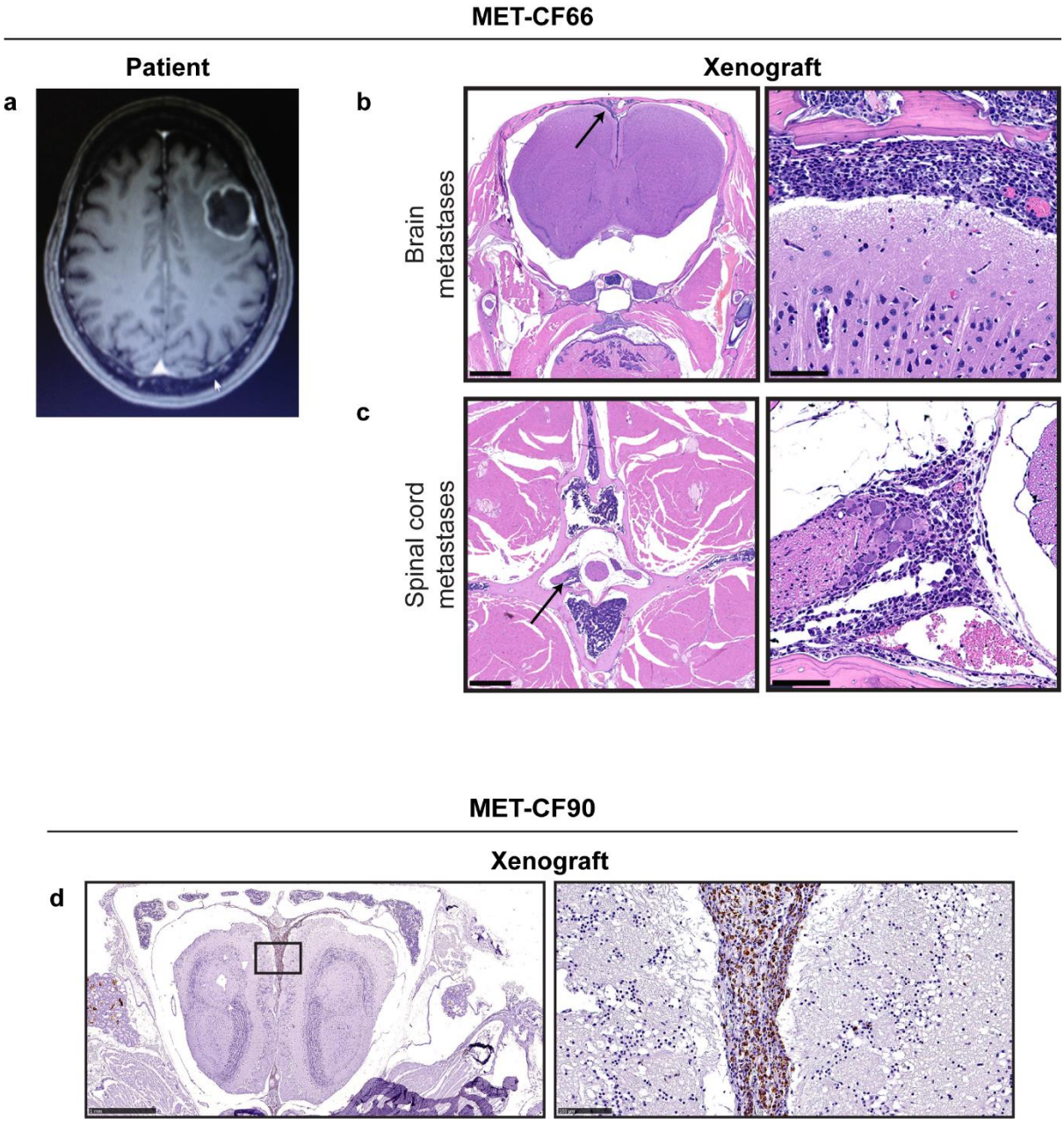

Supplementary Figure 4. Spontaneous CNS leptomeningeal dissemination in flank implanted BMs from lung cancer.
(**A**) Brain MRI, axial T1 contrast-enhanced sequence, of a 66 years-old female patient with a left frontal BM from lung adenocarcinoma (MET-CF66). (**B-C**) H&E staining showing spontaneous leptomeningeal dissemination to the brain and the spinal cord in the matched mouse xenograft. Arrow indicates metastasis's location. (**D**) Representative anti-human mitochondria staining of a mouse brain with leptomeningeal dissemination derived from a 68 years-old patient with a posterior fossa BM from lung adenocarcinoma (MET-CF90). Scale bars: (B) 1mm and 100µm, (C) 1mm and 100µm, (D) 1mm and 100µm. Related to Figure 2.

Supplementary Table 3. Matched patient and mice metastatic sites in intracardiac PDX models.

Primary tumor	Sample ID	Metastases location												
		CNS	Lungs	Liver	Kidney	Suprarenal	Intraperit.	Spleen	Gonads	Orbita	Mandibula	Soft tissues	Bone/Bone marrow	Subcut.
Lung	MET-CF30													
	MET-CF66													
	MET-CF68													
	MET-CF78													
	MET-CF79													
	MET-CF87													
Osteosarcoma	MET-CF65													
Melanoma	MET-CF69													
Colon	MET-CF70													
	MET-CF82													
	MET-CF89													
Bladder	MET-CF29													
Endometrium	MET-CF81													

Red - organs with tumor involvement in the patient; Green - organs with tumor involvement in the mouse; Yellow - organs with tumor involvement in both patient and mouse. Related to Figure 4.

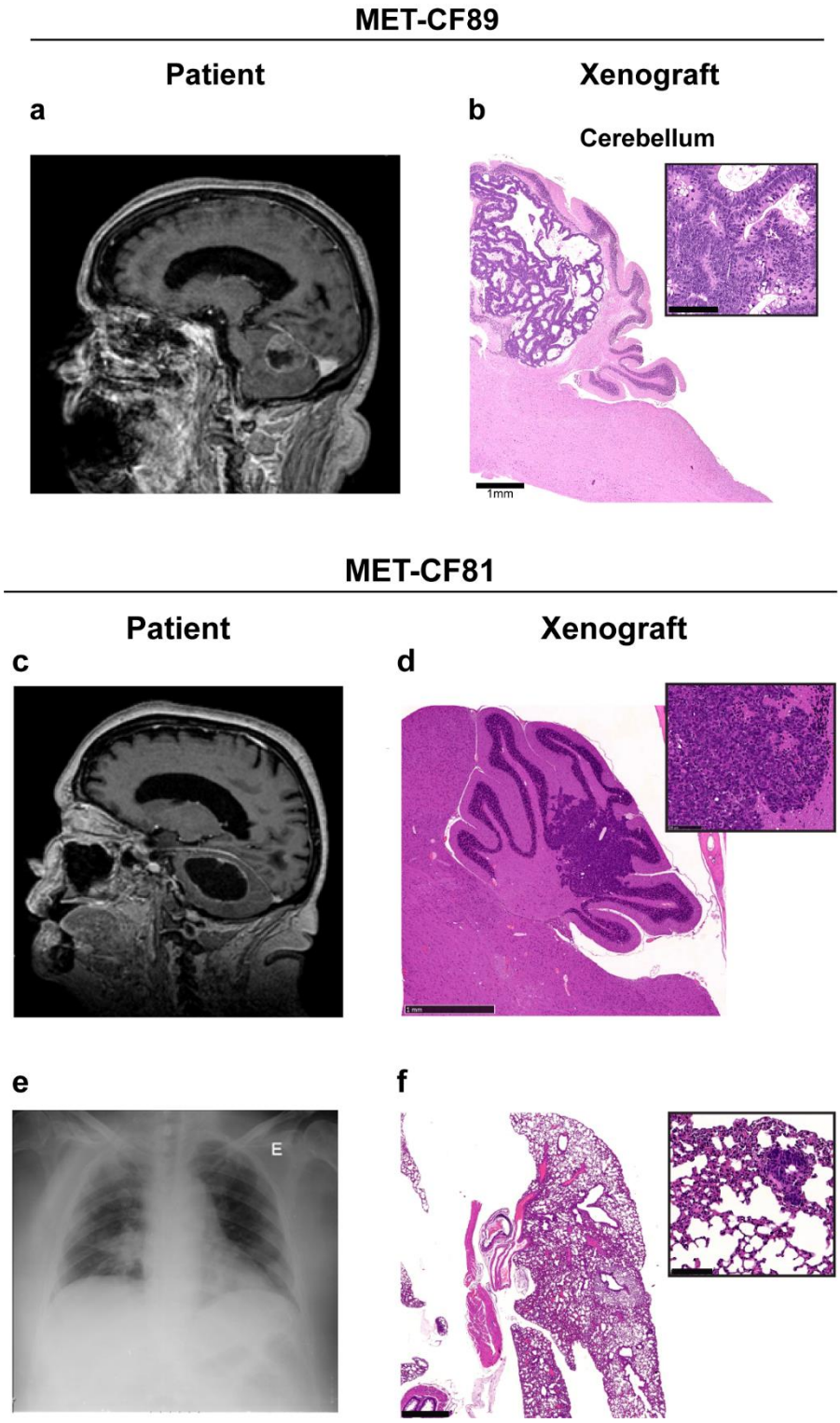

Supplementary Figure 5. Comparison of clinical cases and their matched intracardiac PDXs models. Intracardiac xenograft of a surgically resected cerebellar BM (MET-CF89) from a patient with colon cancer mirrored the intracranial location of the patient's tumor. (**A**) Brain MRI, sagittal T1 contrast-enhanced sequence, of an 81 years-old male patient with a BM in the cerebellum from a colon carcinoma. (**B**) Corresponding H&E staining of a metastasis in the mouse cerebellum.
Representative clinical case of a 67 years-old female patient with metastatic endometrium cancer derived BM (MET-CF81), where the intracardiac xenograft shared two metastatic sites with the donor. (**C**) Brain MRI, sagittal T1 contrast-enhanced sequence, showing a cystic BM in the cerebellum and (**D**) the correspondent H&E staining of the mouse metastasis in the cerebellum. (**E**) Right lung metastases in the patients' chest X Ray and (**F**) the matched lung metastases in the xenograft. Scale bars: (B) 1mm and 100µm, (D) 1mm and 100µm, (F) 1mm and 100µm. Related to Figure 4.

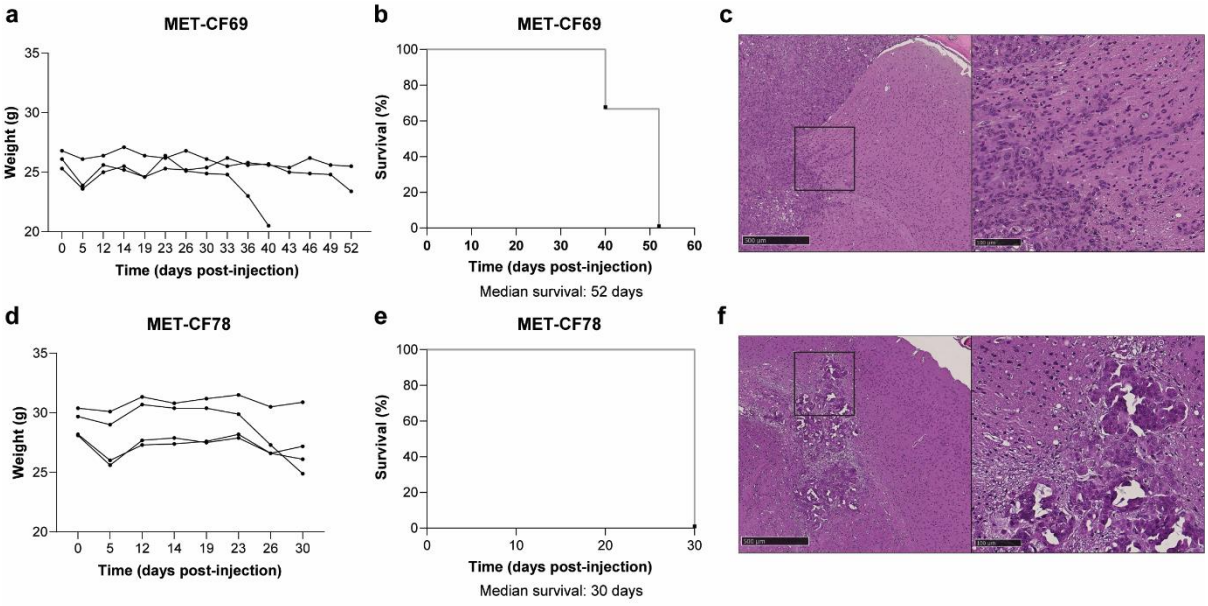

g

PDC	Primary tumor	Histological evaluation				
		Brain invasion	Brain dissemination	Brain stem/cerebellum dissemination	Spinal cord thoracic dissemination	Spinal cord lumbar dissemination
MET-CF69 (N=3)	Melanoma	3/3 (3/3 HI)	0/3	0/3	0/3	0/3
MET-CF78 (N=4)	Lung	4/4 (2/4 HI)	3/4	2/4	2/4	2/4

Supplementary Figure 6. *In vivo* models of orthotopic implanted BMs.
PDCs were established from subcutaneous xenografts of BM samples derived from patients with (**A-C**) a melanoma and (**D-F**) a lung carcinoma. The growth pattern of these PDCs in the brain was assessed after intracranial injection of cells in mice. (**A** and **D**) Body weight variation throughout time, (**B** and **E**) survival curves and (**C** and **F**) H&E sections of brain tumors are shown for each PDC in 5x (left) and 20x (right) amplifications. (**G**) Histological evaluation of H&E sections of mice CNS was performed to evaluate the pattern of brain invasion and dissemination, as well as the dissemination along the spinal cord. Scale bars: (C) 500µm and 100µm, (F) 500µm and 100µm. Related to Figure 6.

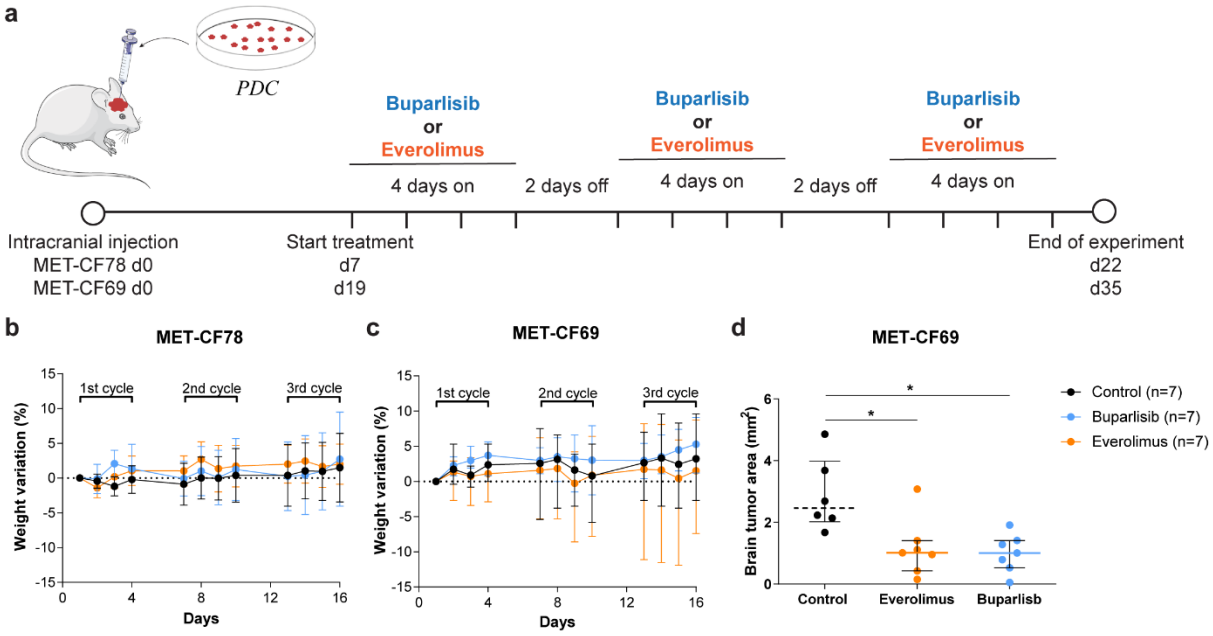

Supplementary Figure 7. Patient-derived xenografts were established by the intracranial injection of PDCs to assess the efficacy of buparlisib and everolimus in vivo.
(**A**) Representative scheme of the treatment evaluation performed in xenografts established by the intracranial injection of PDCs derived from BM samples of a lung (MET-CF78) and a melanoma (MET-CF69) cancer patients. Animals were randomly divided in 3 groups: buparlisib (30mg/kg/day; n=7), everolimus (3mg/kg/day; n=7), and vehicle (5% DMSO/30% PEG300/H_2O; n=7) used as a negative control for comparison. Treatment administration was performed in 3 cycles of therapy with buparlisib and everolimus. Body weight variation was assessed throughout time for (**B**) MET-CF78 and for (**C**) MET-CF69. (**D**) Histological sections of the CNS were evaluated to assess the tumor area in the brain. Data is represented as median with interquartile range. Differences were considered statistically significant for p-values<0.05, according to the Mann-Whitney test. Related to Figure 6.